ChemElectroChem

Review
doi.org/10.1002/celc.202300491

Chemistry Europe
European Chemical Societies Publishing

www.chemelectrochem.org

Carbon Covering Method to Enhance the Storage Capacity of Materials Belonging to the Conversion and Alloy Storage Types

Yuan Mu,[a] Jianke Li,[a] Kun Wang,*[a] Guiying Xu,*[a] Baigang An,[a] and Weimin Zhou*[a]

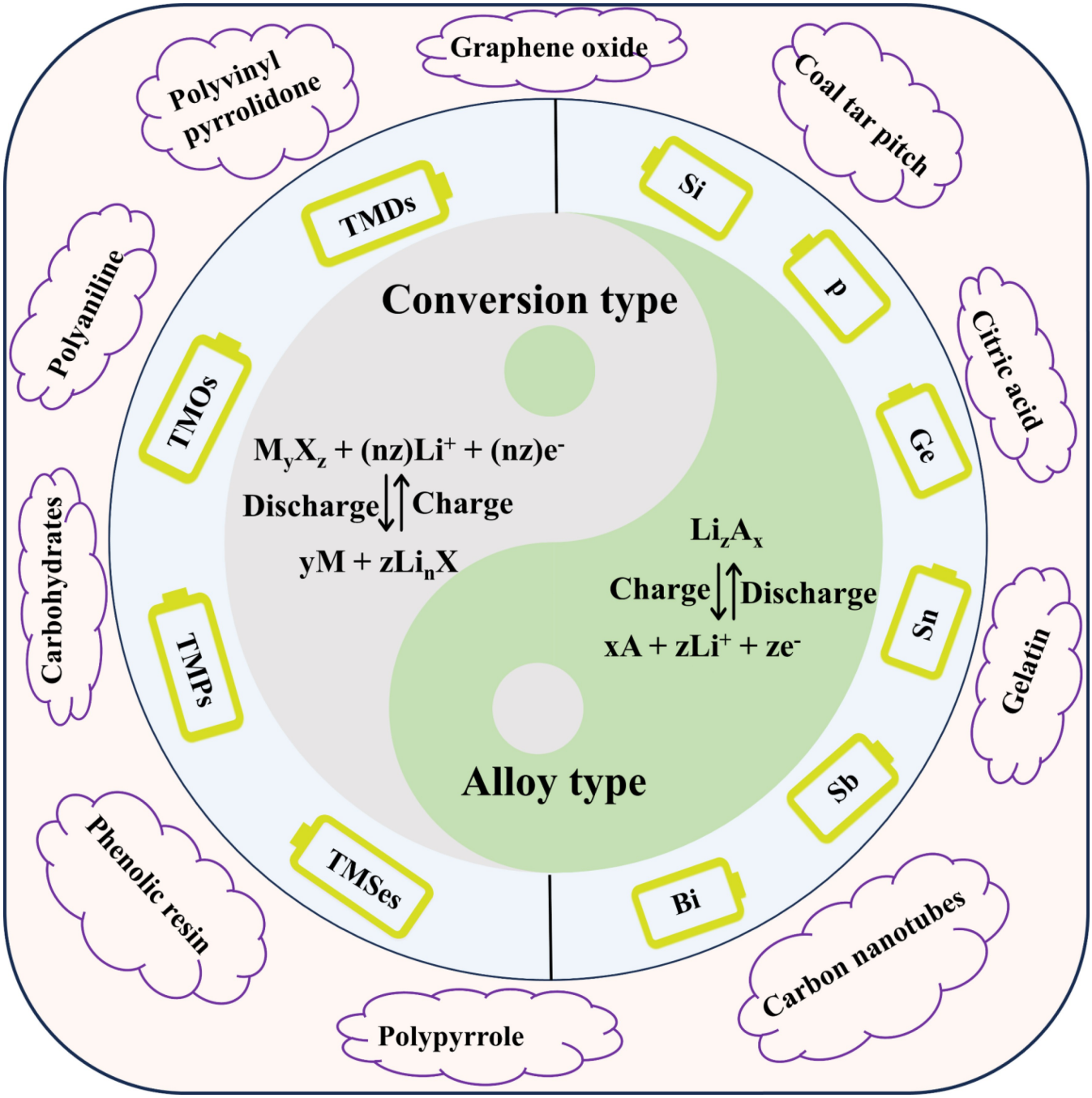

Driven by the development of energy storage systems (EESs), finding alternative anode materials forlithium-ion batteries to replace the general carbon materials is becoming a hot research topic in the world. Using the metal oxides, metal sulfides, metal phosphides, metal selenides belonging to the conversion type and Sn, Sb, Bi, Ge, P and Si belonging to the alloy storage type seems to be a preferred option. Nevertheless, the demerits such as volume expansion and bad conductivity of alternative materials restrict their practical application. Carbon covering is an efficacious strategy to deal with the aforementioned issues because it can restrict the volume expansion and improve the conductivity of the composite materials effectively. This present review paper comprehensively describes the suitable carbon resources and preparation methods for expanding the practical applications of materials belonging to the conversion type and ally type in fabrications of negative electrodes.

1. Introduction

The need for developing alternative energy sources like solar, wind, and tidal energy has become necessary as a result of the substantial air pollution caused by the transitional use of fossil fuels. However, the issue of unstable energy supply of aforementioned new energies restricts their practical applications. Unfolding the energy storage systems (ESSs) provides an effective way to address the above issues in the world.[1] Since the advent of lithium-ion batteries (LIBs) by SONY in 1985, it has made the great progress in the applications of electric vehicles, various electrics and even to some extent grid storage.[2] Recently, some energy storage proposals such as sodium ion batteries (SIBs), thermal energy storage and mechanical energy storage have been advocated widely.[3] Nevertheless, these proposals are in the development stage, and they have not yet achieved large-scale applications. Compared to them, the development of lithium ion batteries is relatively mature and they have reached the industrial production level.[4] Therefore, developing the LIBs still has the practical significance. Additionally, the application of intelligent detection system increases the safety of (ESSs). Thus, it is necessary to develop the storage capacity of electrode materials for LIBs.

In the past 20 years, the positive electrodes of LIBs have been significantly unfolded. The many positive electrodes having high capacity such as $LiCoO_2$ (LCO), $Li(Ni_xMn_yCo_z)O_2$(NMC), $Li(Ni_xCo_yAl_z)O_2$(NCA),and $xLi_2MnO_3\cdot(1\text{-}x)LiMO_2$ are developed remarkably.[5] In contrast, the kinds of negative electrodes are relatively single. The artificial graphite and natural graphite negative electrodes are widely used to assemble the LIBs because of their good conductivity, high reversibility, low cost, and suitable working voltage.[5b,6] Nevertheless, the theoretical capacity of graphite materials is only 372 mAh g^{-1}, which means that it is unable to meet the needs of large-scale energy storage development.[2] In response to the market demand for anode electrode materials with the high energy density, alternative materials for general carbon anode materials should be developed eagerly.

Figure 1 displays the main storage mechanisms of negative electrodes for storing the Li^+. To sum up, it is mainly classified into three types such as intercalation, alloy and conversion types.[7] Except for graphite negative electrodes, the biomass-derived carbons, polymer-derived carbons, MOF-derived carbons and N and S doped carbons are also classified to the intercalation type.[8] These negative carbon materials show the higher storage capacity, compared with the graphite carbons, which is attributed to their modified surfaces, special porous structures and the defects of carbons.[9] However, the demerits such as low initial coulombic efficiency (ICE) and high operating voltage restrict their practical applications.[10]

Metal oxides, metal sulfides, metal phosphide and metal selenide generally embody the characteristics of the conversion storage type.[11] The conversion reaction generally can be written as $M_yX_z + (nz)Li^+ + (nz)e^-$ yM $\leftrightarrow +zLi_nX$.[12] Among them, the M represents the transition metals such as Fe, Co, Ni, et al., and the X are the nonmetallic elements such as S, O, P, and Se. Conversion storage type mainly depends on the aforementioned reaction among two kinds of elements. The oxidation-reduction reactions among the two kinds of elements help to increase the storage capacity of the M_yX_z materials. Thus, these M_yX_z materials have been attracted more attention than ever before. Nevertheless, the shortcomings such as remarkable volume change and poor conductivity should be overcome in the practical applications.[11c,13]

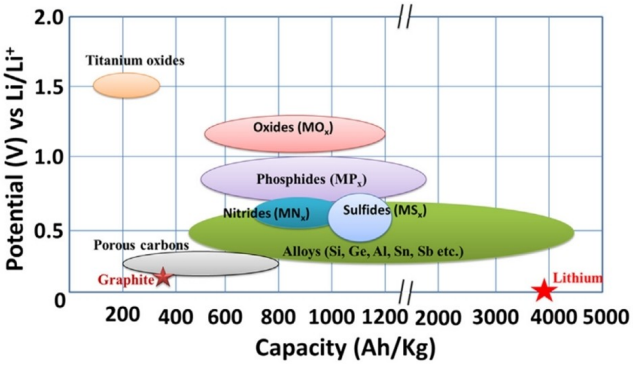

Figure 1. Schematic classification of common anode materials for lithium-ion batteries. Reproduced from Ref. [7] Copyright (2013), with permission from The Authors. Published by Elsevier B.V.

[a] *Y. Mu, J. Li, K. Wang, G. Xu, B. An, W. Zhou*
Key Laboratory of Energy Materials and Electrochemistry Research Liaoning Province, University of Science and Technology Liaoning, No. 189, Qianshan Middle Road, Lishan District, Anshan City, Liaoning Province, Anshan 114051, China
E-mail: aszhou15242870697@163.com
ustl15542731203@163.com
xuguiying751107@163.com

The alloy type is that the Li^+ storage capacity depends on the alloying and dealloying processes which are mainly performed by using the Si, P, Ge, Sn, Sb, and Bi elements.[14] This type is mainly reflected by a reaction of $xA + yLi^+ + ye^- \leftrightarrow Li_yA_x$.[14a] In this reaction, A is the one of elements of Si, P, Ge, Sn, Sb and Bi. The alloy type can markedly increase the storage capacity of LIBs, which can provide a very effective way to address the subject enhancing the energy density of LIBs. Likewise, the pulverization phenomenon of metals by the volume expansion also exists in the charge-discharge process. Additionally, the issues such as bad Li^+diffusionand instability of solid electrolyte interface (SEI) should be solved necessarily.[6,14b]

Covering the carbon materials on the surface of the aforementioned materials belonging to the alloy storage type and conversion type is an effective strategy to address the aforementioned issues. It is attributed to that the carbons can restrict the volume expansion of metals and M_yX_z materials not only, but they can increase the electronic and ion transfer of composites also.[11c,15] The choices of carbon sources are particularly significant in light of the statements above. Associated with the covering experience of our group, the carbon covering strategy in application to enhance the storage capacity of materials belonging to the conversion and alloy types is described as following (Figure 2).

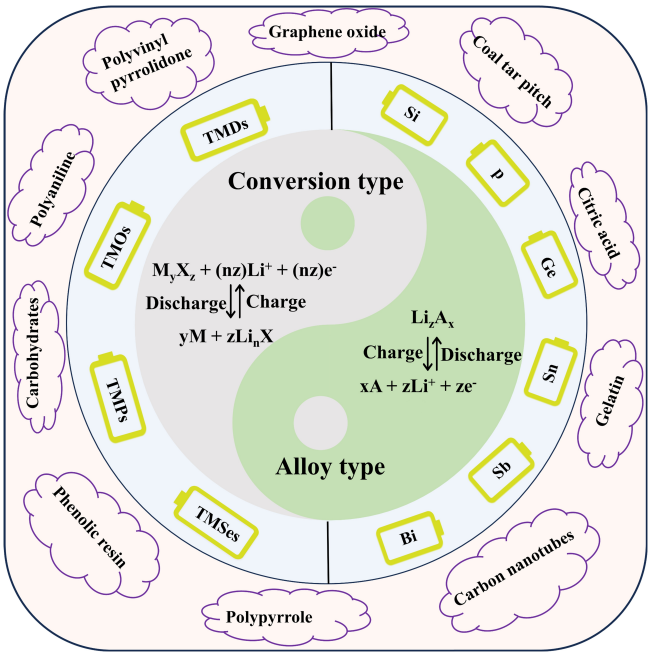

Figure 2. The illustration of carbon sources which are used to enhance the storage capacity of materials belonging to the conversion and alloy storage types.

Yuan Mu received his master's degree in Materials and Chemical Engineering from University of Science and Technology Liaoning in 2020. Currently, he is a Ph.D. candidate under the supervision of Prof. Weimin Zhou at University of Science and Technology Liaoning. His research interests focus on energy storage materials. It mainly includes the negative electrode materials of lithium-ion batteries and sodium-ion batteries.

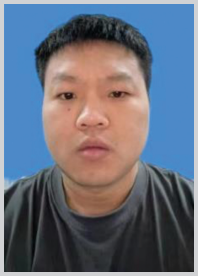

Jianke Li received his master degree from University ofScience and Technology Liaoning, China. He is now studying for his doctorate in University ofScience and Technology Liaoning. His current research focuses on energy storage materials. It mainly includes the negative electrode materials of lithium ion batteries and sodium ion batteries.

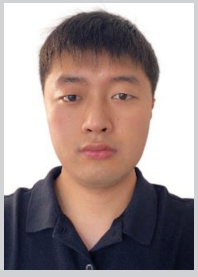

Kun Wang received his Ph.D. degree in Ferrous Metallurgy from University of Science and Technology Liaoning in 2020. He carried out his postdoctoral research at East China University of Science and Technology of Shanghai from 2016 to 2022. Currently, he is a lecturerin the College of Chemical Engineering, University of Science and Technology Liaoning. His research interests focus on advanced electrode materials for lithium-ion batteries and sodiumion batteries.

Guiying Xu received her doctor degree from University of Science and Technology Liaoning, China. She is a associate professor of University of Science and Technology Liaoning. Her current research focuses on new carbon materials for energy storage systems.

Baigang AN is a professor of University of Science and Technology Liaoning, China. He received his Ph.D in Applied Chemistry at Tianjin University in 2003 supervise by Prof. Shizhe SONG.He had ever worked as a research fellow in Tohoku University Japan and a visiting scholar in Michigan University. His current research interests include synthesis and application of nanomaterials in electrochemical storage and conversion of energy.

WeiminZhou is a professor of University of Science and Technology Liaoning, China. He received his Ph.D in Tokyo Institute of Technology in Japan 2009. He carried out his postdoctoral research in Nagaoka University of Technology Japan from 2010 to 2013.His current researchesmainly focus on the electrochemistry, polymer chemistry, coal chemistry and organometallic chemistry.

2. Enhancing the storage capacity of materials belonging to the conversion storage type

As mentioned above, the covering carbon on the surface of M_yX_z materials is the pivotal point in enhancing the electrochemical performance. According to the characteristics of graphene oxide (GO), polyaniline, biomass, coal tar pitch and et al., the combinations of carbons with M_yX_z materials show the complex diversity.[16] The excellent synergy between the covering carbons and M_yX_z is an important key to develop the storage capacity of M_yX_z.

As a two-dimensional carbon material, GO is widely applied in the storage field due to its many merits such as large specific surface area, high mechanical strength, and excellent conductivity.[17] Additionally, the monoatomic layer and unique mechanical property lead GO to have the flex and crimp characteristics.[18] Therefore, the GO can tightly cover the surface of M_yX_z materials in nano sizes, and can bridge them together to form the negative electrode materials with three-dimensional (3D) network structures.[19] It is conceivable that using the sheets of GO or rGO to cover the M_yX_z materials can improve their cycle performance drastically. Meanwhile, the electronic and ion conductivities can also be improved remarkably.[20] Furthermore, in comparison with the monometallic oxides, the cooperative effects among the different metals in the binary oxides with the spinel structure cause that the binary oxides to exhibit the excellent electrochemical performance. Similarly, the demerits such as bad reaction kinetics, poor intrinsic conductivity and volumetric expansion in the charge-discharge processes also restrict their application in assembling the LIBs.[19,21] Tang et al. successfully fabricated the $ZnMn_2O_4$-rGO/CNT composites through the in situ growth of $ZnMn_2O_4$ nanoparticles on the surface of 3D layered rGO and carbon nanotubes (Figure 3a).[22] The constructed 3D layered carbon network enhanced the electronic and ion conductivities. Meanwhile the volumetric expansion of metals was also restrained effectively (Figure 3b, c and e). The $ZnMn_2O_4$-rGO/CNT benefits from the synergies of GO and nanotubes, resulting in a storage capacity of 606 mAh g^{-1} at 1.0 A g^{-1} after cycling 1000 times (Figure 3d). The capacity retention of $ZnMn_2O_4$-rGO/CNT is the 83 %. Nevertheless, the cost of production requires careful consideration.

Polyvinyl pyrrolidone (PVP) as a non-ionic polymer is an excellent carbon resource since it can easily dissolve in water and most organic solvents. Using the PVP to perform the carbons which are covered on the surface of M_yX_z materials can realize the N-doping concurrently by the N in the PVP. The carbons obtained by carbonizations of PVP can easily construct the 2D or 3D conductive network on the surfaces of M_yX_z.[23] In this covering process, the PVP can effectively avoid the agglomeration phenomenon among the M_yX_z, for the ketone groups of PVP have the coordination property to the Cu^{2+} and Ni^{2+}.[24] CuO has drawn more attention owing to its high theoretical capacity, cost-effectiveness, and environmentally-friendly.[25] Using the hydrothermal method, Zhang et al. successfully covered the carbons on the surface of CuO by the PVP, and those CuO/C composite materials were placed on the surface of the nickel foam (NF) (Figure 4).[26] The finally fabricated electrode (CuO/C/NF) without using binders shows the high storage capacity (505.0 mAh g^{-1})at 2.0 A g^{-1}, after cycling 800 cycles. It is attributed to that the covered carbons enhanced the stability and conductivity of CuO/C/NF composite materials due to the formation of mesoporous pores of covered carbons.

The π conjugated bonds in polyaniline(PANI) cause that the carbons obtained by the carbonizations of PANI to possess the tremendous conductivity.[27] Meanwhile, the PANI possesses the advantages of simple synthesis, high thermal stability and

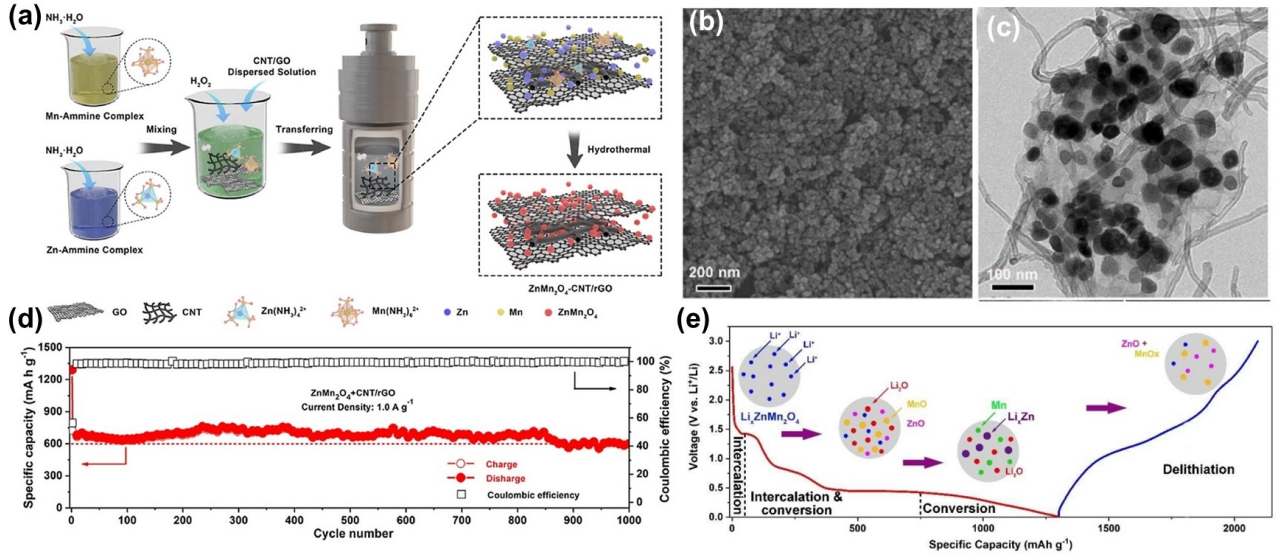

Figure 3. (a) schematic illustration of the preparation process, (b) SEM, and (c) TEM images of $ZnMn_2O_4$-CNT/rGO composite. (d) Cyclic stability at a current rate of 1.0 A g^{-1} and (e) the schematic illustration of the energy storage mechanisms of $ZnMn_2O_4$-CNT/rGO electrode. Reproduced from Ref. [22] Copyright (2020), with permission from Elsevier B.V.

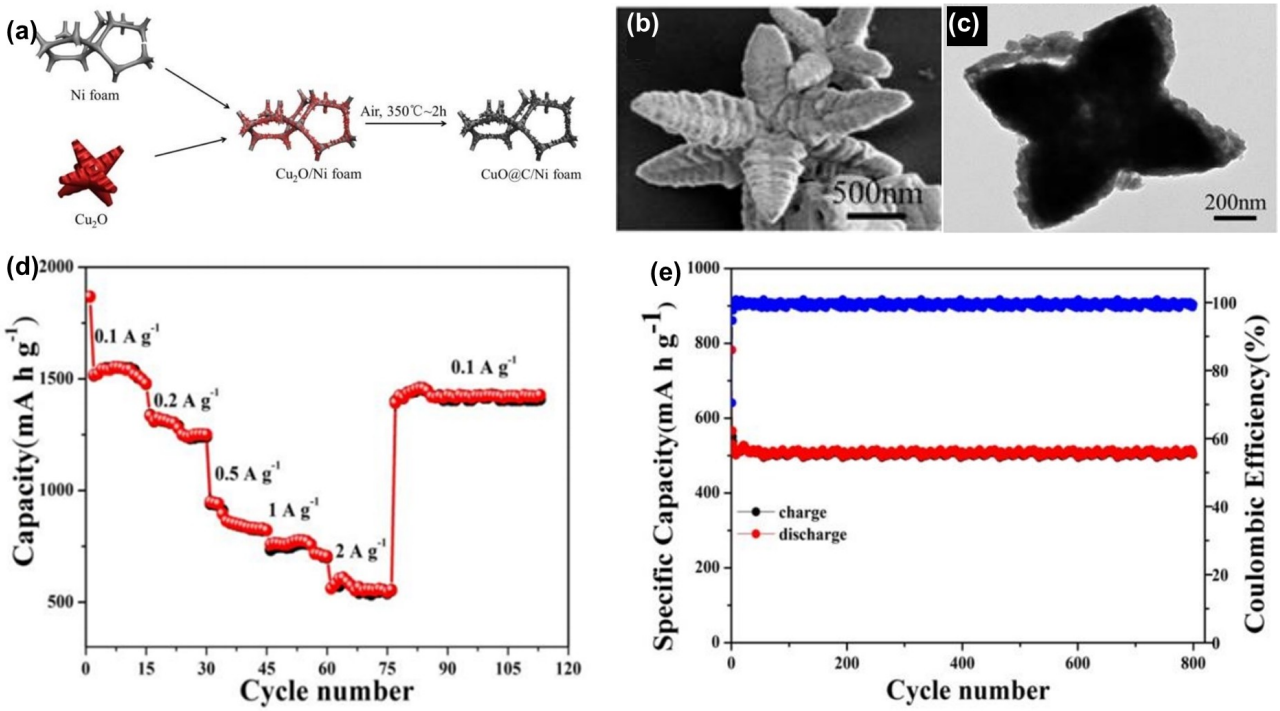

Figure 4. (a) schematic illustration of the preparation process, (b) SEM, and (c) TEM images of CuO/C/NF composite. (d) Rate capability performance and (e) cycling performance at the current density of 2 $A g^{-1}$ of CuO/C/NF composite. Reproduced from Ref. [26] Copyright (2020), with permission from Wiley-VCH GmbH.

excellent mechanical flexibility. Thus, PANI has garnered great attention as a carbon resource.[28] To increase the structural stability, enhance ionic/electronic transport and buffer volume changes of high entropy oxide (HEO) during the cycling, the carbons obtained by PANI precursor were covered on the surface of micrometer-sized high entropy oxide (HEO-M) by the high-energy ball milling method.[29] Meanwhile, it is found that the covering carbons can prevent the side reactions between electrolyte and electrode materials, and suppress the over-production of SEI in long cycling process. After carrying out the electrochemical evaluations, the storage capacity of HEO-MP is 822.7 $mAh g^{-1}$ at 0.5 $A g^{-1}$, after 100 cycles. These results indicate that the PANI is an effective carbon source for developing the storage capacity of materials belonging to the conversion storage type.

Hard carbons obtained by the biomass are often used in lithium-ion batteries because of their low cost and natural abundance.[30] Carbohydrates (glucose, sucrose, fructose, cellulose and starch) having more oxygen-containing functional groups are widely used to cover the M_yX_z materials.[31] Studies have shown that the transition metal phosphides (TMPs) own the more fabulous storage capacity than that of general metal oxides.[32] Likewise, the dramatic volume expansion in charge-discharge processes and complex preparation processes restrict the practical application of TMPs.[33] Based on the aforementioned descriptions, Liu et al. fabricated the Co-gluconate precursor having a uniform spherical morphology by the solvothermal method (Figure 5a).[34] After carrying out the carbonization and phosphorization, the CoP(CoP@C) composite materials were fabricated successfully. In this composite material, CoP in nanosize was covered by carbons very well, resulting in the increasing conductivity, reactive sites of CoP, and the remarkably shortened Li^+ transmission pathway (Figure 5b–c)). As a result, this CoP@C composite material shows the storage capacity of 483.4 $mAh g^{-1}$ at 0.5 $A g^{-1}$ when carrying out the charge-discharge 1000 cycles (Figure 5d).

Except for sugar precursors, the biopolymer gelatin precursor with the advantages of low cost and environment-friendly is becoming an excellent carbon resource gradually. The abundant amino, carboxyl and carbonyl groups on the main chains of bio polymer gelatin make it possible to be dissolved only in hot water but not in cold water.[35] This characteristic property of biopolymer gelatin was widely used to fabricate the M_yX_z@C storage materials belonging to the conversion storage type.[36] Additionally, the existence of groups containing the N elements facilely produces the N-doping in the carbonization, which can increase the pseudocapacitance behavior of electrodes.[37] Iron based sulfides possess the excellent advantages such as high theoretical capacity, cost-effectiveness and environmentally friendliness.[38] In a report by Li et al., the Fe_9S_{10}@C composite materials are facilely fabricated by using the gelatin, $FeSO_4 \cdot 7H_2O$ and $Na_2S \cdot 9H_2O$ by one-step method.[39] Nanocrystallization of iron sulfides can increase the reaction sites and shorten Li^+ diffusion distance to accelerate the reaction kinetic rate between Li^+ and iron sulfides.[40] Since the gelatin possesses several hydroxyl groups that are favored for dispersing Fe^{2+} of $FeSO_4 \cdot 7H_2O$, it is used as a carbon source for better dispersing the fabricated Fe_9S_{10} in the carbon substrates(Fig-

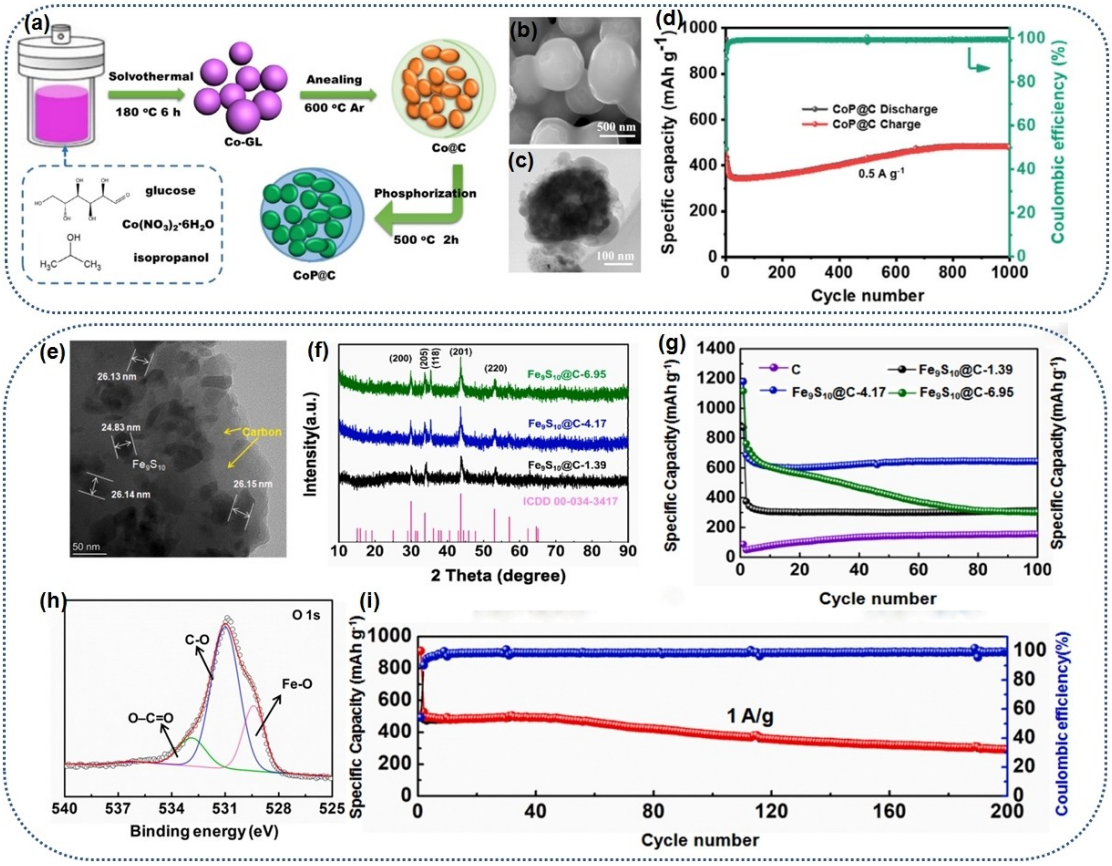

Figure 5. (a) schematic illustration of the preparation process, (b) SEM image, (c) TEM image and (d) the long-term cycle stability of CoP@C composite. Reproduced from Ref. [34] Copyright (2021), with permission from Wiley-VCH GmbH. (e) TEM images, (f) XRD pattern and (h) XPS spectra of Fe_9S_{10}@C-4.17 material. (g) Cycling performances of Fe_9S_{10}@C composites. (i) the long-term cycle stability of Fe_9S_{10}@C-4.17 composite. Reproduced from Ref. [39] Copyright (2023), with permission from Elsevier B.V.

ure 5e). The Fe_9S_{10} in nano sizes in carbon substrates can remarkably increase the reaction kinetic rate between Li^+ and iron sulfides, leading to the enhancement of electrochemical performances of Fe_9S_{10}@C materials. It is verified that the formations of Fe–O bonds between the gelatin-based carbons and Fe_9S_{10} can construct the conductive network, which effectively boosts the charge transfer around Fe_9S_{10} and further develops the electrochemical performance of Fe_9S_{10} (Figure 5h). Furthermore, it is interestingly found that the gelatin influenced the formation of Fe_9S_{10} in the Fe_9S_{10}@C composites during preparations (Figure 5f). After carrying out electrochemical measurements, it is observed that the fabricated Fe_9S_{10}@C material shows the excellent storage capacity (645.0 $mAhg^{-1}$) at 0.1 $A\,g^{-1}$, after cycling 100 times (Figure 5g). The Fe_9S_{10}@C material also exhibits the high storage capacity at a large current density. For instance, Fe_9S_{10}@C can still exhibit the storage capacity of 298.5 $mAhg^{-1}$, when carrying out the charge-discharge 200 cycles at 1 $A\,g^{-1}$(Figure 5i). The reason for these excellent electrochemical performance can also be attributed to the unique pore structure of the Fe_9S_{10}@C composites. The existence of massive mesoporous and macropores is beneficial for Li^+ transfer, causing an improvement in the rate performance. In addition, other SnO_2@C composite materials fabricated by using the gelatin carbon resource were reported by Wang et al.[41] In this work, the SnO_2@C composite materials were fabricated by reaction using the gelatin, $SnCl_4 \cdot 5H_2O$ and aqueous $NH_3 \cdot H_2O$ by one-step method. Compared to the SnO_2, the SnO_2@C shows the improved electrochemical performance. After 500 cycles at a current density of 0.1 $A\,g^{-1}$, the storage capacity of SnO_2@C is still 397.7 $mAh\,g^{-1}$. The improvement electrochemical performance is generally attributed to the formation of mesoporous of covered carbons. The aforementioned reports strongly support to that the gelatin is a useful carbon source to enhance the electrochemical performance of M_yX_z composite materials.

Recently, coal tar pitch (CTP) which is converted from coal has drawn more attention, for it has more advantages such as abundant reserves, strong cost leadership and high carbon contents (>90%).[42] Additionally, a lot of polycyclic aromatic hydrocarbons (PAHs) in coal tar pitch can cause the carbons obtained by carbonizations of coal tar pitches to have tremendous conductivity. As an anode material with characteristics of high quality and low cost, the researches about iron oxides (Fe_2O_3, Fe_3O_4 and FeO) have been developed quickly.[43] Wang et al. dissolved the coal tar pitches in the pyridine solution, and used the obtained pyridine solution to cover the Fe_3O_4 (Figure 6a).[43c] After carbonization, it is observed that the FeO/C composite materials were synthesized by controlling the

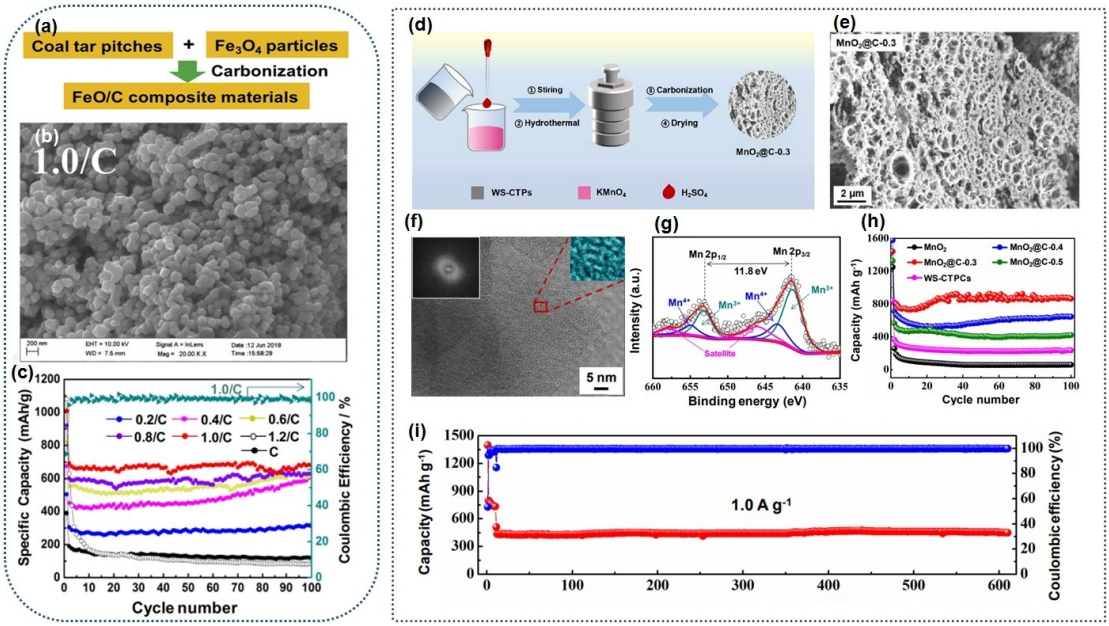

Figure 6. (a) Schematic diagram of the preparation, (b) SEM image and (c) Cycling performances of FeO/C composite. Reproduced from Ref. [43c] Copyright (2019), with permission from Hydrogen Energy Publications LLC. Published by Elsevier Ltd. (d)Schematic illustration, (e) SEM image, (f) HRTEM image and (g) XPS spectra of MnO_2@C-0.3 material. (h) Cycling performances at 0.1 A g^{-1} of MnO_2@C-0.3 material. (i) the long-term cycle stability of MnO2@C-0.3 composite. Reproduced from Ref. [44] Copyright (2023), with permission from Science China Press.

dosages of coal tar pitch and Fe_3O_4 particles in the reactive cases, and their electrochemical performance was evaluated in detail ((Figure 6b–c)). It is found that the FeO/C (1.0/C) manifests the fabulous electrochemical performance. As an example, the 1.0/C anode still has the storage capacity (679 mAh g^{-1}) at 0.1 A g^{-1}, after cycling 100 times. This report reveals that coal tar pitch as a useful carbon source can be used to cover the M_yX_z materials. Considering the enormous cost advantage, the CTP as a carbon source shows the huge applicable perspective.

To increase the covering efficiency and decrease the environmental burden, the water soluble coal tar pitches (WS-CTPs) were developed and used to cover the M_yX_z materials as a carbon resource because they possess the good water solubility and a lot of PAHs contents. The WS-CTPs can be simply fabricated by using the mixtures of sulfuric acid (concentration: 98%) and nitric acid (concentration: 65%). Liu et al. successfully fabricated the MnO_2@C materials by using the WS-CTPs and $KMnO_4$ by the hydrothermal method (Figure 6d).[44] It is interestingly observed that MnO_2 exists in the MnO_2@C materials in an amorphous state, and the MnO_2@C composite materials show different structures with conversing the dosages of WS-CTPs (Figure 6e–g). In addition, the produced mesoporous structures of carbons facilitate the Li^+ diffusion, leading to the improvement of reaction kinetics. After performing the electrochemical evaluations, it is found that the fabricated MnO_2@C-0.3 shows the storage capacity at 865.2 mAh g^{-1} after 100 cycles at a current density of 0.1 A $g^{<M-1}$ (Figure 6h). In addition, the storage capacity of MnO_2@C-0.3 still maintains 450.3 mAh g^{-1}, after cycling 600 cycles at a current density of 1.0 A g^{-1} (Figure 6i). Li et al.also fabricated the V_2O_3@C composite materialsby using the WS-CTPs, $V_2O_5$and $H_2C_2O_4 \cdot 2H_2O$.[45] The fabricated V_2O_3@C-2.0 composite materials also exhibit the excellent storage capacity of 580.2 mAh g^{-1} after 100 cycles at 0.1 A g^{-1}. Meanwhile, the V_2O_3@C-2.0 also exhibits the high storage capacity of 234.0 mAh g^{-1} at 5.0 A g^{-1} after 500 cycles. The aforementioned experiments indicate that WS-CTPs are the one of effective carbon sources to enhance the storage capacity of M_yX_z materials.

In addition to the carbon resources mentioned earlier, the carbon nanotubes (CNTs), citric acid, phenolic resin and other carbon sources are often used as other carbon sources to cover the M_yX_z materials.[27,46] Likewise, the electrochemical performance of M_yX_z@C materials has been greatly improved. Table 1 summarizes the recent progress in the electrochemical properties of conversion type LIBs anode materials covered by carbon, respectively.

At the end of this section, the preparation methods, carbon morphology, porosity and specific surface of M_yX_z materials were illustrated in the Table 2. It is found that the combinations of the three factors of carbon sources, metals or M_yX_z and synthesis methods cause that the prepared composite materials have the different structures. In our presented studies, it is interestingly found that the M_yX_z@C materials have the similar porosity or specific surface, when the target products of M_yX_z@C materials have the similar molecular structure, carbon resources and preparation methods are coincident. Therefore, by comparing carbon sources, synthesis methods and molecular structures of M_yX_z, the structure characteristics of target M_yX_z@C materials can be roughly predicted (Table 2).

Table 1. The electrochemical properties of conversion-type LIBs anodematerials covered by different carbon.

Carbon source	Typical examples	Current density ($mA\,g^{-1}$)	Capacity ($mAh\,g^{-1}$) @cycle number	Ref.
GO	FeP@C/rGO	100	949.7@100	[63]
	G⊥FP@C-NA	500	1009.0@500	[64]
	$Co_{1-x}S$/rGO	2500	527.2@107	[65]
	H-Co_3O_4/P-RGO	200	1016.0@200	[66]
	GO/Fe_3O_4	100	1023.0@250	[67]
	GO–Fe3O4	1000	411.0@100	[68]
CNTs	$CoFe_2O_4$@CNT	100	243.0@60	[69]
	NiO/CNTs	723	692.3@100	[70]
PANI	HEO-MP	4000	261.0@3200	[29]
	PANI/Co_3O_4–CuO	100	681.0@60	[71]
	Gr−Fe_3O_4−PANI	100	949.0@250	[72]
	h-Fe_3O_4@PANI	100	956@50	[43a]
	GR/PANI/CuS NC	100	1255@2500	[73]
PVP	CuO/C/NF	2000	505.0@800	[26]
	MoS_2-PVP@NC	1000	607.1@300	[74]
	MFO/C-3	100	783.0@100	[75]
	MnO_x@C–Cu	400	1030@350	[76]
	$MnMoO_4$@C	100	1050@200	[77]
Carbohydrates	1T-MoS_2/C	1000	870@300	[78]
	CoP@C	500	483.4@1000	[34]
	S 6–8	200	1297.1@200	[79]
	Fe_9S_{10}@C	100	645.0@100	[39]
Gelatin	$ZnFe_2O_4$/C	200	955.9@100	[80]
	SnO_2@C	100	397.7@500	[41]
	VS_2-NC	100	1061.0@200	[81]
	1.0/C	100	679.0@100	[43c]
	MnO_2@C-0.3	100	865.2@100	[44]
CTP	V_2O_3@C-2.0	100	580.2@100	[45]
	ZCO-CTP5	500	1104.3@400	[82]
	MnO_2/PGC36	1000	692.0@400	[83]
	Fe_3O_4@C-500	200	718.4@500	[84]
Citric acid	FL-MNO@C	2000	481.0@2000	[85]
	ZnO/NC	98.7	1047.0@100	[86]
	porous carbon/α-Fe_2O_3	100	1272.0@200	[87]
Phenolic resin	Fe_3O_4@C-1.3	100	915.0@120	[88]
	PCMS@MnO	2000	527.0@2000	[89]

3. Enhancing the storage capacity of materials belonging to the alloy storage type

The metals (Sn, Sb, Ge and Bi) and non-metals (Si and P) are generally classified to the alloy storage type.[14a,47] Because of the fact that these anodes manifest a significantly fabulous storage capacity, they are widely expected to be alternative materials in the application of ESS. Likewise, the issue of alloy-based materials broken in charge-discharge processes also needs to be solved. It is considerable that the carbon covering method is also one of the effective methods to address the aforementioned issue.

In the 1970s, a number of researchers carried out the studies on the Si as a negative material. It is observed that Si can form the alloys of $Li_{12}Si_7$, $Li_{14}Si_6$, $Li_{13}Si_4$, and $Li_{22}Si_5$ with the extremely high storage capacity (4200 $mAh\,g^{-1}$) in the discharge processes.[48] The merits of cost-effectiveness and environmental friendly characteristics lead plenty of researchers and industries to consider that the Si is the best negative material instead of the carbon anode. However, the low conductivity ($10^{-3}\,S\,cm^{-1}$) and Li^+ diffusion coefficient (10^{-14} ~$10^{-13}\,cm^2\,s^{-1}$) diminish its reaction kinetics.[49] Meanwhile, the issue of the immense volume expansion of Si in alloying-dealloying processes is solved necessarily. Additionally, the volume expansion of Si leads the solid electrolyte interface (SEI) continuously to be destructed and formed in Li^+ charge-discharge processes, which remarkably diminishes the coulombic efficiency and rate performance of Si.[50]

To address the aforementioned issues, covering the carbon on the surface of Si becomes one of the effective ideas. Thus, the studies about Si/C negative materials are very popular in the world, for the carbons can restrict volume expansion not only, but they can increase the conductivity of composites also. For instance, Peng et al., used the gelatin and template method to fabricate carbons with the 2D network structures, and then covered these carbons on the surface of Si (Figure 7a–f)).[51] The fabricated Si@GCNS composite materials possess the remarkably improved electrochemical performance. After undergoing 400 cycles, it shows the storage capacity of 1583 $mAh\,g^{-1}$ at 2 $A\,g^{-1}$(Figure 7g). In addition, after the soft-packing batteries are assembled by using the $LiFePO_4$ as a positive electrode and Si@GCNS as a negative electrode, they also exhibit the excellent cycling performance. For instance, these batteries show high capacity retention (89.8%) at 1 A g-1 after 300 times, and the energy density of batteries is ~460 Wh kg^{-1}(Figure 7h). The remarkably improved electrochemical performance can be attributed to the formation of 2D carbon nanosheets fabricated by gelatins because these nanosheets can boost the Li^+ transfer not only, but the structural stability of Si is increased markedly.

Except for the silicon, the Li^+ can insert the P to form the Li_3P, causing phosphide possesses the high theoretical capacity (2595 $mAh\,g^{-1}$).[52] Thus, the phosphide as a highly commercialized negative electrode material is also expected to be utilized in fabrications of anodes of LIBs. Over the past decades, the storage capacity of red phosphorus and black scale were widely surveyed by a lot of research groups.[52,53] However, the white phosphorus can not be applied in the application of electrodes owing to its volatility, virulence and spontaneous combustion characteristics.[54] In addition, the demerits such as the poor cycling performance, volume expansion (300%) and slow lithiation reaction kinetics cause that the structures of P based materials should be improved in practical applications.[52,54] Mixing the P with carbons having the high conductivity is a facile strategy to develop the storage capacity of P. For instance, Li et al., used the tannin acid (TA) and pyrrole (Py) to construct the multi-layer carbons on the surface of P based carbon nanotube (P-CNT) by an in situ polymerization method.[55] A lot of oxygen atoms in TA possess the strong adsorptive ability for P and its compounds (Li_xP_s), leading to TA

Table 2. The illustrations of preparation methods, carbon morphology, porosity and specific surface of conversion-type LIBs anode materials.

Carbon source	Typical examples	Preparation methods	Carbon morphology	Pore size (average) (nm)	Pore volume ($cm^3\ g^{-1}$)	Specific surface ($m^2\ g^{-1}$)	Ref.
	FeP@C/rGO	Solvothermal	Nanosheets	3.4		452.7	[63]
GO	H-Co_3O_4/P-RGO	Freeze-dried	Nanosheets	4.0		230.0	[66]
	pG/SnO_x/C	Ice bath	Nanosheets	1.7	0.800	531.0	[113]
CNTs	MoO_3-(CNT)	Ultrasonication + Ice bath	Nanorods	~40.0	0.072	19.8	[27]
PANI	h-Fe_3O_4@PANI	Hydrothermal + Ice bath	Nanospheres	5.0~30.0		109.4	[43a]
	GR/PANI/CuS	Ice bath	Ultrathin sheet			57.8	[73]
PVP	MoS_2-PVP@NC	Hydrothermal	Yarn ball-like	2.0~50.0	0.220	22.4	[74]
	MnMoO4@C	Hydrothermal	Nanorods	1.6		20.1	[77]
Carbohydrates	1T-MoS_2/C	Hydrothermal	Nanosheets	~2.0	0.363	134.4	[78]
	S 6–8	Spray Pyrolysis	Spherical- Shape	0.9~400.0		144.8	[79]
	Fe_9S_{10} @C-4.17	Water-solvent	Lump	21.5	0.086	25.5	[39]
Gelatin	ZFO/C-450	Water bath	Nanosheets	60.0		16.2	[80]
	SnO_2@C-40	Water-solvent	Lump	3.1~12.3	0.085	34.6	[41]
	VS_2-NC	Freeze drying	Nanosheets	6.9		69.7	[81]
	MnO_2@C-0.3	Hydrothermal	Lump	3.4~34.0	0.590	84.7	[44]
CTP	V_2O_3@C-2	Hydrothermal	Lump	2.5~35.0	0.370	111.0	[45]
	MnO_2/PGC-36	In situ Precipitation	Carbon Skeleton	1.5~16.0	1.045	190	[83]
Citric acid	Fe_3O_4@C-500	Carbonization	Lump	~3.9		96.6	[84]
	ZnO/NC	Hydrothermal	Skein-shaped	2.4~2.6		86.0	[86]
Phenolic resin	carbon/α-Fe_2O_3	Self-assembly	Finger-like	3.8~100.0	0.280	89.0	[87]
	PCMS@MnO	Hydrothermal	Pomegranate-like	2.9~4.7	0.120	56.4	[89]

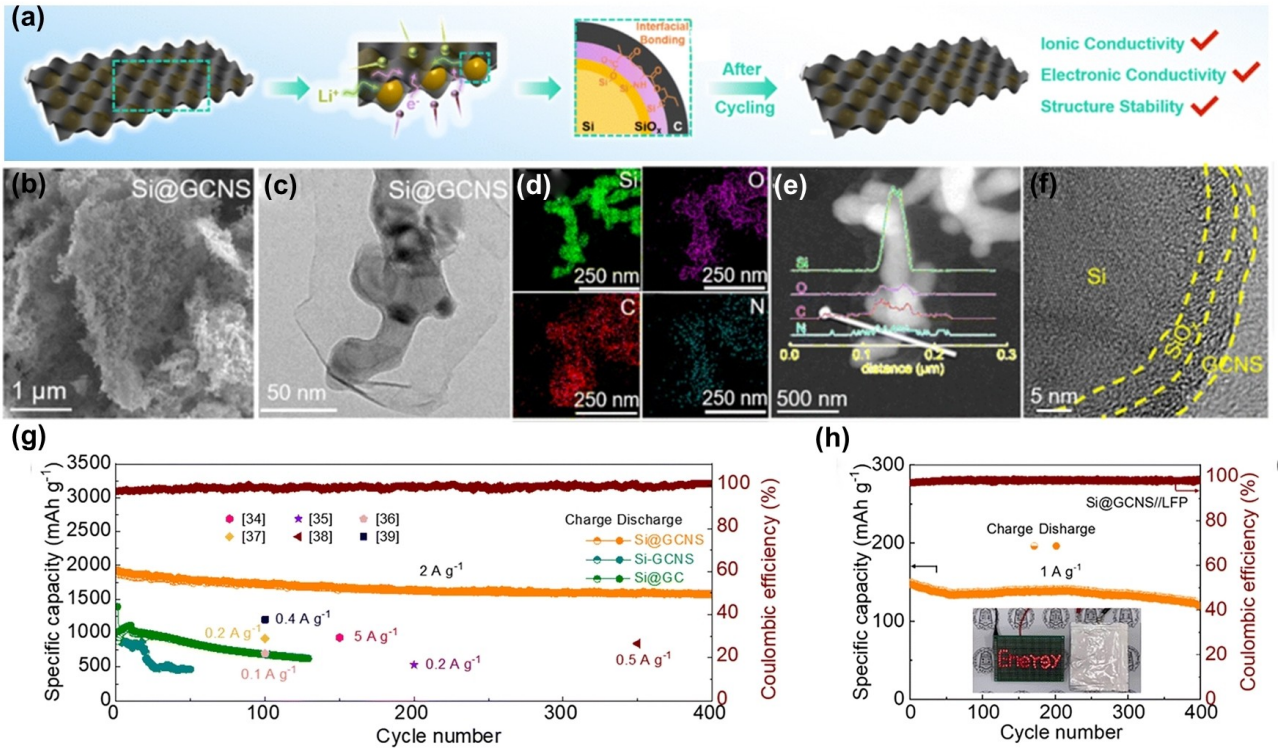

Figure 7. (a) Abridged general view of synthesis process, (b) SEM image, (c) TEM image, (d)areal elemental mapping images, (e) line-scan profile and (f) HRTEM image of Si@GCNS composite. (g) the long-term cycle stability of Si@GCNS material. (h) Cycling performances at 1.0 A g^{-1} for pouch cell. Reproduced from Ref. [51] Copyright (2022), with permission from Royal Society of Chemistry.

could be coated on the surface of P very well. The carbons obtained by carbonizations of Py exhibit the tremendous conductivity. As a result, the carbons formed by co-carbonizations of TA and Pycan buffer the volume expansion of P not only, but the conductivity can be improved also. The special structureof P-CNT@TA-PPy composite material leads it to exhibit the extremely excellent cycling performance (790 mAh g^{-1}) at a large charge current density of 1.0 A g^{-1}, after cycling 100 times. Meanwhile, the capacity retention ratio of P-CNT@TA-PPy is 77.8%.

Similar to phosphorus, germanium can react with lithium to form $Li_{22}Ge_5$ (or $Li_{15}Ge_4$) to produce a theoretical specific capacity of 1624 mAh g^{-1} (or 1384 $mAhg^{-1}$), and it also possesses good electrical conductivity (2000 S m^{-1}) and Li^+ diffusivity, which makes the germanium a promising anode material for lithium-ion batteries.[56] Well-designed nanostructures of germanium/carbon composites have been successfully used to suppress the large volume expansion of germanium during lithium storage (370%).[15a,57] By the in-situ reduction method, Chen et al., successfully dispersed the Ge nano particles on the frameworks of 3D interconnected porous graphene (3DPG) using the polystyrene (PS) ball as a template and GeO_2 as a Ge source (Figure 8a–e).[57] Due to the contribution of the three-dimensional porous graphene framework, the synthesized Ge/3D-PG composite material has a specific surface area of 119 $m^2 g^{-1}$. Compared with pure Ge negative electrodes, the Ge/3D-PG composite material with a higher specific surface area is more conducive to expanding the electrical contact area between the electrolyte and electrode material, providing more active sites for storing the Li^+. Therefore, the fabricated Ge/3DPG materials exhibit the excellent cycling performance. For instance, after cycling 250 times, the storage capacity of Ge/3DPG achieves931.0 mAh g^{-1} at 0.5 C (Figure 8f). It is ascribed to the improved conductivity, and the restricted volume expansion of Geby the 3DPG. The 3D porous structures play the role to improve the reaction kinetics. Getting benefit from the excellent synergy between Ge nano particles and 3D porous graphene frameworks, the Ge/3DPG exhibits tremendous electrochemical performance. These results indicate that the three-dimensional porous graphene is an excellent covering carbon to enhance the storage capacity of metals belonging to the alloy storage type.

In comparison with the Si, P and Ge, the Sn, Sb and Bi own the more excellent conductivities(Table 3), which leads the Sn, Sb and Bi elements to possess the more excellent rate performances.[58] Furthermore, the volume expansion of Sn, Sb and Bi in charge-discharge processes is relatively small, causing these anodes to have the fabulous cycling performance. Among them, Sn can form the alloy of $Li_{22}Sn_5$ to contribute the theoretical capacity of 990 mAh g^{-1}.[15a] Meanwhile, through the formation of the Li_3Sb alloy, the Sb exhibits thetheoretical capacity of 660 mAh g^{-1}.[14a] Recently, the Sb becomes the more attractive electrode as an material due to its suitable work potential (~0.8 V vs. Li^+/Li).[14b] Meanwhile, Bi is also attracted exceedingly, owing to its plenty of advantages such as excellent conductivity, cost-effectiveness, non-toxic properties and suitable work potential. Moreover, in view of its high mass density, Bi generally displays the markedly high volume capacity of 3800 mAh cm^{-3}.[58] Although these three elements of Sn, Sb,

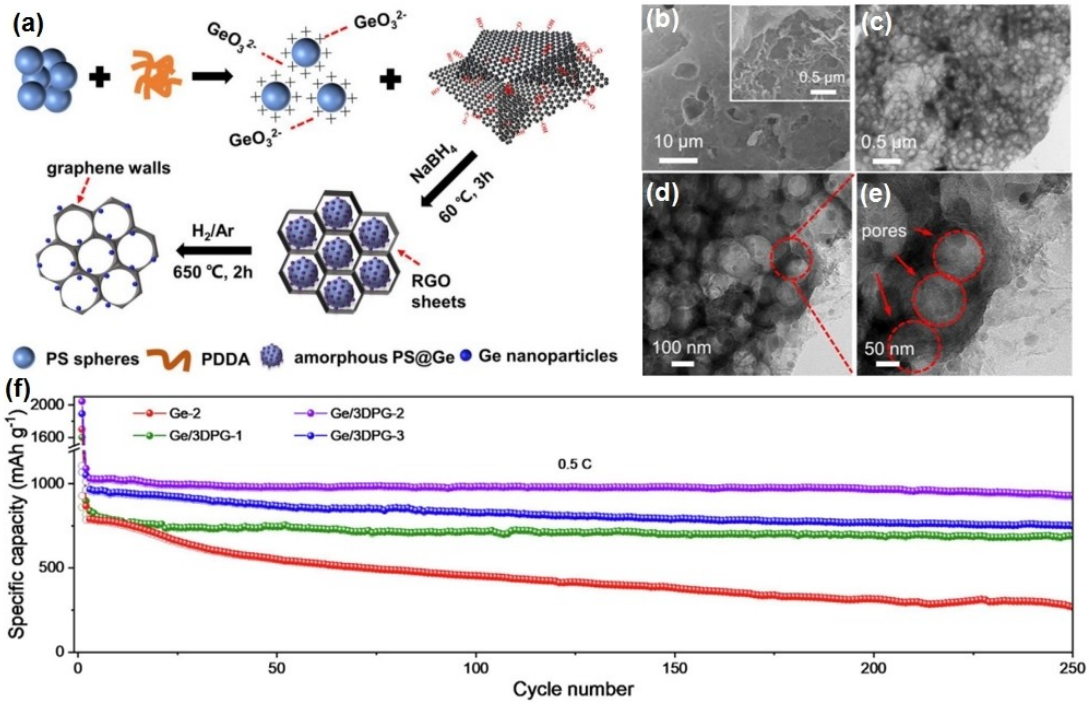

Figure 8. (a) schematic illustration of the synthesis process, (b) SEM and (c–e) TEM images, (d) the long-term cycle stability of Ge/3DPG material. Reproduced from Ref. [57] Copyright (2021), with permission from Science Press and Dalian Institute of Chemical Physics, Chinese Academy of Sciences. Published by ELSEVIER B.V. and Science Press.

Table 3. Comparison of physicochemical properties of typical alloy-type anode materials.

Element	Electrical conductivity ($S\,m^{-1}$)	Density ($g\,cm^{-3}$)	Theoretical capacity ($mAh\,g^{-1}$)	Ref.
Si	$2.5*10^{-4}$	2.35	4200	[48, 90]
P(red)	$1.0*10^{-12}$	2.34	2595	[52, 90]
P(black)	$3.0*10^{4}$	2.70	2595	[52, 90]
Ge	$2.0*10^{3}$	5.32	1624	[56]
Sn	$9.1*10^{6}$	7.28	994	[56, 90]
Sb	$2.6*10^{6}$	6.68	660	[60, 90]
Bi	$7.7*10^{5}$	9.78	385	[14b, 90]

and Bi possess excellent storage capacity, the common issue of the dramatic volume expansion of metals can not be ignored. Through constructing the interfaces between the carbons and metals, the aforementioned common issue also be solved well.[15a] For example, Sun et al., designed and fabricated a C/Sn/C composite material with the hollow sphere sandwich structureby using the hard template method (Figure 9(a, b)).[59] In this composite material, the Sn nano particles were completely encapsulated into the concentric N-doping carbon shell. The nano space between the double carbon layers easily solve the issue brought by the volume expansion of Sn in the formation of $Li_{22}Sn_5$ alloy. This addresses the pulverization problem of Sn very well (Figure 9c–d). As a result, many merits such as the high storage capacity of Sn, excellent conductivity of carbons, large contact area of the electrolyte with electrodes and high contributions of pseudocapacitance lead that the synthesized C/Sn/C composite materials to manifest theexcellent electrochemical performance. As an example, the C/Sn/C exhibits the high storage capacity of 1100 $mAh\,g^{-1}$ at a current density of 0.1 $A\,g^{-1}$, when the charge-discharge processes were conducted 130 times (Figure 9e).

To address the issue of volume expansion better, the double covering method is a good strategy encouraged by Zheng et al.[60] On the basis of double covering idea, Mu et al., synthesized the Sb@rGO@NSC (Sb covered by rGO and N, S doped carbons) by co-carbonizations using the $SbCl_3$, GO, glucose, ammonium citrate and sulfocarbamide (Figure 9f).[61] It is observed that the 3D porous structures of Sb@rGO@NSC were constructed by the surrounding of lamellar structures (Figure 9g–h)). The TEM measurements were further used to confirm the structures of Sb@rGO@NSC-0.3 (Figure 9i). Figure 9j demonstrates that the Sb particles in sizes around 20–30 nm are covered by the carbons thoroughly, suggesting that Sb dispersed in carbon substrates very well. The fabricated Sb@rGO@NSC materials display the exceedingly excellent electrochemical performance. For instance, the Sb@rGO@NSC-0.3 exhibits a high storage capacity (1121.2 $mAh\,g^{-1}$) at 0.5 $A\,g^{-1}$, over cycling 500 times (Figure 9k). The storage capacity of Sb@rGO@NSC-0.3 has 721.1 $mAh\,g^{-1}$ and 343.3 $mAh\,g^{-1}$, even after carrying out the cycles 1000 times with current densities set as 1.0 $A\,g^{-1}$ and 5.0 $A\,g^{-1}$, respectively. It is considerable that the excellent electrochemical performance is attributed to the fabulous dispersions of Sb particles with nano sizes in carbon substrates and formations of 3D hierarchical porous structures of the Sb@rGO@NSC-0.3.

On the basis of the same double concept, Wu et al., prepared the Sb@C/EG materials by using the citric acid, expanded graphite and $SbCl_3$.[62] In Sb@C/EG composite materials, it is found that a lot of Sb nanoparticles are embedded on the surface of carbon blocks, and the nano Sb particles can be goodly dispersed in graphite nanosheet layers having the high specific surface area, excellent conductivity, and flexibility. The characteristic structures of Sb@C/EG can avoid the volume expansion of Sb nanoparticles. Meanwhile, the agglomeration phenomenon of Sb nanoparticles can be avoided very well. As a result, the Sb@C/EG shows the excellent cycling and rate performance. After cycling 600 times, the Sb@C/EG still exhibits the storage capacity (486$mAhg^{-1}$) at a current density of 1.0 $A\,g^{-1}$.

In conclusion, the carbon covering method is an efficacious way to enhance the storage capacity of materials belonging to the alloy storage type. The relation reports were illustrated as shown in Table 4.

4. Summary and Outlook

To satisfy the demands for ESSs, developing electrodes having a significantly high storage capacity is becoming an urgent task for enterprises and research institutions. Conversion-type and alloy-type negative electrodes have become potential commercial negative electrode materials due to their advantages such as high theoretical capacity and abundant resources. The Carbon covering method is an effective way to address the demerits of low conductivity, bad reversibility and cycling performance of materials belonging to the conversion type and alloy type. Therefore, studies on searching the suitable carbon sources are becoming extremely hot topics. To better develop the synergistic effect between the covering carbons and metal or M_yX_z (metal oxides, metal sulfides, metal phosphides, metal selenides, and so on), the carbon contents in composite materials should be adjusted seriously because high carbon contents will decrease the storage capacity. Meanwhile, according to the selections of carbon sources and kinds of metal or M_yX_z, the selections about the synthesization method are also pivotal.

Finally, the conversion and alloy type negative electrodes are still under investigation towards practical application. On the whole, we expect that the following points should be improved in future. (i) The relatively high charge-discharge plateaus should be decreased by the creative design of material fabrications. (ii) The cost of carbons should be decreased for the practical application. (iii) The initial coulombic efficiency (ICE) should be increased, while maintaining the high storage capacity of composite materials. With the fast development of the studies regarding the materials belonging to the conversion and alloy types, we believe that those materials will be widely applied in the near future.

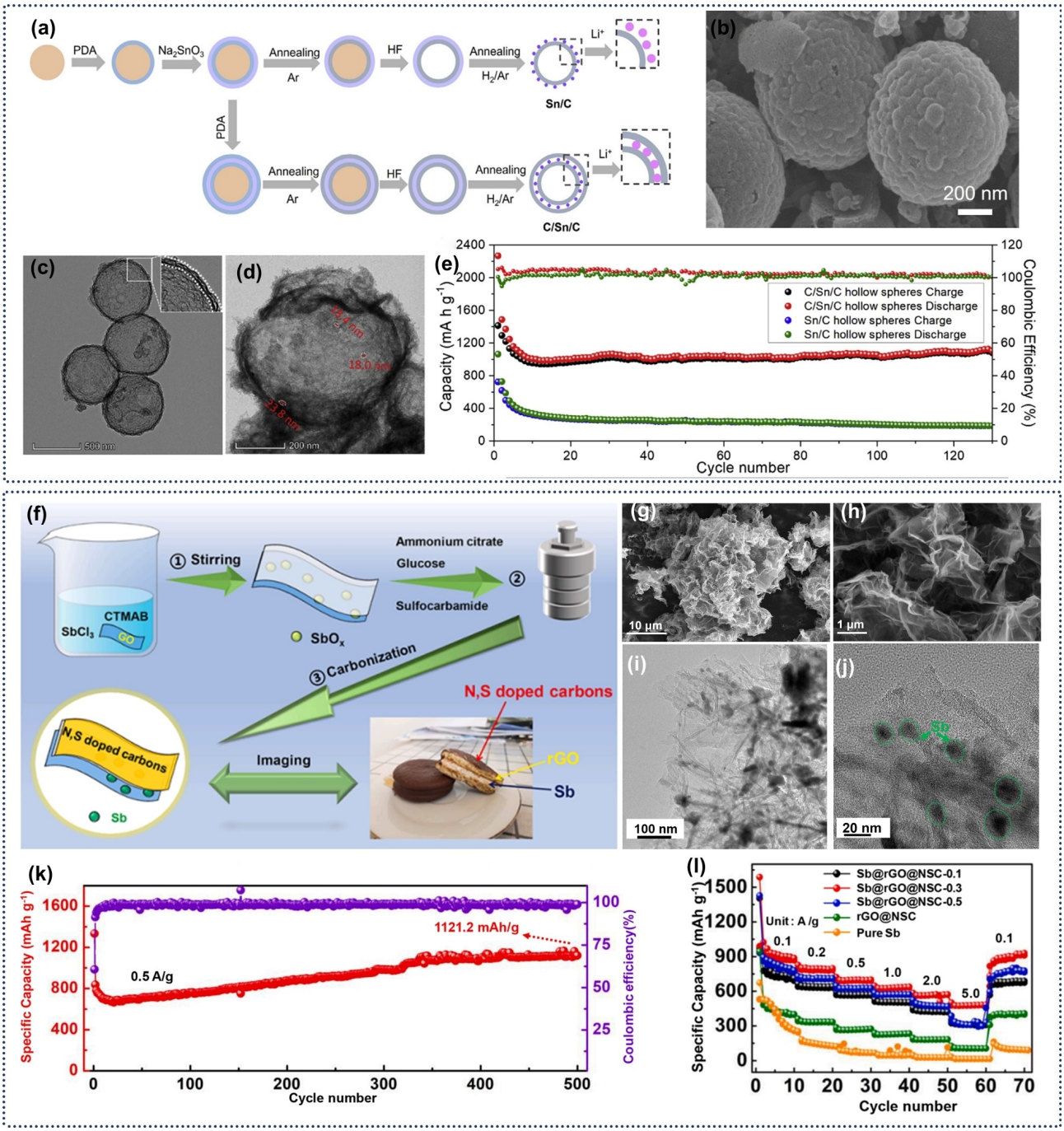

Figure 9. (a) Schematic diagram of the preparation, (b) SEM and (c, d) TEM images of C/Sn/C composite. (e) Cycling performances at 0.1 A g^{-1} of C/Sn/C composite. Reproduced from Ref. [59] Copyright (2021), with permission from Published by Elsevier Ltd. (f) Schematic illustration, (g, h) SEM images and (i, j) TEM images of Sb@rGO@NSC-0.3 material. (k) Cycling performances at 0.5 A g^{-1} and (l) rate capability performance of Sb@rGO@NSC-0.3 composite. Reproduced from Ref. [61] Copyright (2021), with permission from Elsevier Ltd.

Acknowledgements

We are grateful to the support of University of Science and Technology Liaoning (601009816-39), LJKQZ2021126 and 2017RC03. This work obtains the support by the Liaoning Province Education Department of China (Grant No.601009887-16). This work is partly supported with the project supported by the National Natural Science Foundation of China (Grant No. 51672117 and 51672118).

Conflict of Interests

The authors declare no conflict of interest.

Table 4. The electrochemical properties of various alloy-type anode materials for LiBs.

Typical examples	Current density ($mA\,g^{-1}$)	Capacity ($mAh\,g^{-1}$) @cycle number	Capacity retention (%)	Ref.
Si@GCNS	2000	1583.0@400	83.4	[51]
Graphene/C@Si	200	1182.0@240	89.5	[91]
10SiZGC	1000	600.0@500		[92]
Si@C@CNTs	500	968.0@500	88.0	[93]
@u-Si	420	3300.0@100	90.0	[94]
H-SiNS/C	2000	1040@500	90.4	[95]
P-CNT@TA-PPy	1000	790.0@100	77.8	[55]
BPC	6240	1593.2@100	81.0	[96]
RP-C_H	250	690.7@200	78.6	[97]
BP@CNTs	500	757.3@650		[98]
Ge/3DPG–2	800	931.0@250	85.3	[57]
Ge@C-rGO	100	1183.0@200	76.0	[99]
rGO/Ge/rGO	1600	1085.0@500		[100]
C/Sn/C	100	1100.0@130	78.0	[59]
am-Sn@C	1000	510.0@500		[101]
Sn@C	1000	1116.3@550		[102]
G-HCF-Sn	1000	1048.0@1000		[103]
NPHPC–G@Sn	200	1099.0@500	95.0	[104]
Sb@N-C	200	602.8@300	92.7	[105]
Sb@N-CM	200	695.6@190	100.3	[106]
Sb@C	50	525.0@100	77.0	[107]
Sb/C/G-400	500	592.0@400	88.9	[47b]
C/Sb10	100	466.2@200	78.3	[108]
Sb/C	200	565.0@100	91.5	[109]
CCNs@BiNs	250	322.0@500		[110]
Bi@C	100	233.0@350	74.0	[111]
Bi@CF	1000	306.0@900	72.5	[112]

Data Availability Statement

The data that support the findings of this study are available on request from the corresponding author. The data are not publicly available due to privacy or ethical restrictions.

Keywords: Negative electrode · LIBs · Conversion storage type · Alloy storage type · Energy storage systems (ESSs)

[1] a) M. Chen, Y. Zhang, G. Xing, S.-L. Chou, Y. Tang, *Energy Environ. Sci.* **2021**, *14*, 3323–3351; b) M. Li, J. Lu, Z. Chen, K. Amine, *Adv. Mater.* **2018**, *30*, 1800561; c) Z. Zhu, T. Jiang, M. Ali, Y. Meng, Y. Jin, Y. Cui, W. Chen, *Chem. Rev.* **2022**, *122*, 16610–16751.
[2] a) J. W. Choi, D. Aurbach, *Nat. Rev. Mater.* **2016**, *1*, 16013; b) A. Manthiram, *ACS Cent. Sci.* **2017**, *3*, 1063–1069; c) J. Li, J. Fleetwood, W. B. Hawley, W. Kays, *Chem. Rev.* **2022**, *122*, 903–956.
[3] M. S. Ziegler, *Joule* **2021**, *5*, 1925–1927.
[4] J. Xiang, Y. Wei, Y. Zhong, Y. Yang, H. Cheng, L. Yuan, H. Xu, Y. Huang, *Adv. Mater.* **2022**, *34*, 2200912.
[5] a) W. Li, B. Song, A. Manthiram, *Chem. Soc. Rev.* **2017**, *46*, 3006–3059; b) B. E. Murdock, K. E. Toghill, N. Tapia-Ruiz, *Adv. Energy Mater.* **2021**, *11*, 2102028; c) J. Xiang, Y. Wei, Y. Zhong, Y. Yang, H. Cheng, L. Yuan, H. Xu, Y. Huang, *Adv. Mater.* **2022**, *34*, 2200912.
[6] S. Li, K. Wang, G. Zhang, S. Li, Y. Xu, X. Zhang, X. Zhang, S. Zheng, X. Sun, Y. Ma, *Adv. Funct. Mater.* **2022**, *32*, 2200796.
[7] S. Goriparti, E. Miele, F. De Angelis, E. Di Fabrizio, R. P. Zaccaria, C. Capiglia, *J. Power Sources* **2014**, *257*, 421–443.
[8] L. Li, D. Zhang, J. Deng, Y. Gou, J. Fang, H. Cui, Y. Zhao, M. Cao, *Carbon* **2021**, *183*, 721–734.
[9] a) M. Jiang, Y. Ma, J. Chen, W. Jiang, J. Yang, *Nanoscale* **2021**, *13*, 3937–3947; b) M. Shaker, A. A. S. Ghazvini, T. Shahalizade, M. A. Gaho, A. Mumtaz, S. Javanmardi, R. Riahifar, X. Meng, Z. Jin, Q. Ge, *New. Carbon. Mater.* **2023**, *38*, 247–278.
[10] A. Rajkamal, R. Thapa, *Adv. Mater. Technol.* **2019**, *4*, 1900307.
[11] a) S. Li, K. Wang, G. Zhang, S. Li, Y. Xu, X. Zhang, X. Zhang, S. Zheng, X. Sun, Y. Ma, *Adv. Funct. Mater.* **2022**, *32*, 2200796; b) K. Roy, A. Banerjee, S. Ogale, *ACS Appl. Mater. Interfaces* **2022**, *14*, 20326–20348; c) Y. Lu, L. Yu, X. W. Lou, *Chem* **2018**, *4*, 972–996; d) Y. Shuang, L. Qinghao, D. Xiao, W. Qiang, *J. Energy Storage* **2023**, *61*, 106716.
[12] X. Hao, L. Huijun, W. Xiaomin, *ChemElectroChem* **2023**, *10*, e202201151.
[13] J. Cui, H. Zheng, K. He, *Adv. Mater.* **2020**, *33*, 2000699.
[14] a) J. Asenbauer, A. Varzi, S. Passerini, D. Bresser, *J. Power Sources* **2020**, *473*, 228583; b) J. S. Corsi, S. S. Welborn, E. A. Stach, E. Detsi, *ACS Energy Lett.* **2021**, *6*, 1749–1756; c) A. M. Divakaran, M. Minakshi, P. A. Bahri, S. Paul, P. Kumari, A. M. Divakaran, K. N. Manjunatha, *Prog. Solid State Chem.* **2020**, *62*, 100298.
[15] a) X.-Y. Li, J.-K. Qu, H.-Y. Yin, *Rare Met.* **2020**, *40*, 329–352; b) Q. Yan, S.-T. Ko, A. Dawson, D. Agyeman-Budu, G. Whang, Y. Zhao, M. Qin, B. S. Dunn, J. N. Weker, S. H. Tolbert, J. Luo, *Cell Rep. Phys. Sci.* **2021**, *3*, 100694.
[16] a) Y. Kong, Y. Luo, J. Ma, J. Tang, Y. Huang, M. Zhou, S. Han, *ACS Appl. Energ. Mater.* **2022**, *5*, 5010–5017; b) X. Wang, Y. Liu, H. Han, Y. Zhao, W. Ma, H. Sun, *Sustain. Energy Fuels* **2017**, *1*, 915–922; c) H. Liu, S.-H. Luo, S.-X. Yan, Q. Wang, D.-B. Hu, Y.-L. Wang, J. Feng, T.-F. Yi, *Compos. B. Eng.* **2019**, *164*, 576–582.
[17] a) J. Bi, Z. Du, J. Sun, Y. Liu, K. Wang, H. Du, W. Ai, W. Huang, *Adv. Mater.* **2023**, *35*, 2210734; b) K. Wang, D. Ju, G. Xu, B. Han, M. Chai, Y. Wang, L. Li, X. Zhang, M. Ucida, W. Zhou, *Sci. China Technol. Sci.* **2020**, *63*, 2709–2716.
[18] M. R. Al Hassan, A. Sen, T. Zaman, M. S. Mostari, *Mater. Today Chem.* **2019**, *11*, 225–243.
[19] H. Bin, Z. Yao, S. Zhu, C. Zhu, H. Pan, Z. Chen, C. Wolverton, D. Zhang, *J. Alloys Compd.* **2017**, *659*, 1223–1230.
[20] X. Yang, J. Qiu, M. Liu, H. Ming, H. Zhang, M. Li, S. Zhang, T. Zhang, *J. Alloys Compd.* **2020**, *824*, 153945.
[21] L. Li, G. Jiang, J. Ma, *Mater. Res. Bull.* **2018**, *104*, 53–59.
[22] Q. Tang, Y. Shi, Z. Ding, T. Wu, J. Wu, V. Mattick, Q. Yuan, H. Yu, K. Huang, *Electrochim. Acta* **2020**, *338*, 135853.
[23] Y. Dong, Y. Li, H. Shi, J. Qin, S. Zheng, R. He, Z.-S. Wu, *Carbon* **2020**, *159*, 213–220.
[24] J. Bai, B. Zhao, X. Wang, H. Ma, K. Li, Z. Fang, H. Li, J. Dai, X. Zhu, Y. Sun, *J. Power Sources* **2020**, *465*, 228282.
[25] Y. Tan, Z. Jia, J. Sun, Y. Wang, Z. Cui, X. Guo, *J. Mater. Chem. A* **2017**, *5*, 24139–24144.
[26] R. Zhang, X. Li, L. Ni, A. Xie, P. Li, Y. Shen, L. Lao, *ChemElectroChem* **2020**, *7*, 4038–4046.
[27] L. Kiran, M. K. Aydınol, A. Ahmad, S. S. Shah, D. Bahtiyar, M. I. Shahzad, S. M. Eldin, A. A. A. Bahajjaj, *Molecules* **2023**, *28*, 3319.
[28] A. T. Dipak, P. G. Ketan, V. K. Vishnu, E. S. Makrand, C. S. Mahesh, J. Hyungil, H. Sung-Hwan, S. Ramphal, *J. Mater. Sci. Mater. Electron.* **2022**, *33*, 18452–18463.
[29] J.-Z. Yen, Y.-C. Yang, H.-Y. Tuan, *Chem. Eng. J.* **2022**, *450*, 137924.
[30] L. Xie, C. Tang, Z. Bi, M. Song, Y. Fan, C. Yan, X. Li, F. Su, Q. Zhang, C. Chen, *Adv. Energy Mater.* **2021**, *11*,2101650.
[31] a) B. Guan, W. Sun, Y. Wang, *Electrochim. Acta* **2016**, *190*, 354–359; b) G. Li, X. Wang, X. Ma, *J. Energy Chem.* **2013**, *22*, 357–362; c) F. Qin, H. Hu, Y. Jiang, K. Zhang, Z. Fang, Y. Lai, J. Li, *J. Electroanal. Chem.* **2018**, *823*, 67–72; d) C.-U. Jeong, N. Umirov, D.-H. Jung, D.-H. Seo, B.-M. Lee, B.-S. Choi, S.-S. Kim, J.-H. Choi, *J. Power Sources* **2021**, *506*, 230050.
[32] Y. Zhang, L. Liu, L. Zhao, C. Hou, M. Huang, H. Algadi, D. Li, Q. Xia, J. Wang, Z. Zhou, X. Han, Y. Long, Y. Li, Z. Zhang, Y. Liu, *Adv. Compos. Hybrid Mater.* **2022**, *5*, 2601–2610.
[33] G. Xia, J. Su, M. Li, P. Jiang, Y. Yang, Q. Chen, *J. Mater. Chem. A* **2017**, *5*, 10321–10327.
[34] H. Lu, R. Qian, T. Yao, C. Li, L. Li, H. Wang, *Energy Technol.* **2021**, *9*, 2100605.

[35] a) A. E. Danks, M. J. Hollamby, B. Hammouda, D. C. Fletcher, F. Johnston-Banks, S. E. Rogers, Z. Schnepp, *J. Mater. Chem. A* **2017**, *5*, 11644–11651; b) N. Yang, R. Shao, Z. Zhang, M. Dou, J. Niu, F. Wang, *Carbon* **2021**, *178*, 775–782.
[36] X. Men, T. Wang, B. Xu, Z. Kong, X. Liu, A. Fu, Y. Li, P. Guo, Y.-G. Guo, H. Li, X. S. Zhao, *Electrochim. Acta* **2019**, *324*, 134850.
[37] H. Du, C. Yuan, K. Huang, W. Wang, K. Zhang, B. Geng, *J. Mater. Chem. A* **2017**, *5*, 5342–5350.
[38] J. Li, G. Xu, K. Wang, B. Han, L. Li, Y. Wang, D. Ju, M. Chai, D. Zhang, W. Zhou, *Electrochemistry* **2020**, *88*, 380–386.
[39] J. Li, G. Xu, X. Miao, B. Han, K. Wu, K. Wang, B. An, D. Ju, M. Chai, W. Zhou, *J. Alloys Compd.* **2023**, *946*, 169442.
[40] a) Q. Tang, Q. Jiang, T. Wu, T. Wu, Z. Ding, J. Wu, H. Yu, K. Huang, *ACS Appl. Mater. Interfaces* **2020**, *12*, 52888–52898; b) J. Zhao, Y. Zhang, Y. Wang, H. Li, Y. Peng, *J. Energy Chem.* **2018**, *27*, 1536–1554.
[41] S. Wang, G. Xu, K. Wang, B. Han, Y. Wang, L. Li, D. Ju, M. Chai, D. Zhang, W. Zhou, *Current Research in Green and Sustainable Chemistry* **2021**, *4*, 100099.
[42] P. Zuo, S. Qu, W. Shen, *J. Energy Chem.* **2018**, *34*, 186–207.
[43] a) X. Wang, Y. Liu, H. Han, Y. Zhao, W. Ma, H. Sun, *Sustain. Energy Fuels* **2017**, *1*, 915–922; b) Y. Li, Y. Huang, Y. Zheng, R. Huang, J. Yao, *J. Power Sources* **2019**,*416*, 62–71; c) K. Wang, D. Ju, G. Xu, Y. Wang, S. Chen, J. Zhang, Y. Wu, W. Zhou, *Int. J. Hydrogen Energy* **2019**, *44*, 25199–25206.
[44] B. Liu, K. Wang, Z. Guo, B. Han, G. Xu, D. Ju, B. An, Y. Li, Z. Ni, W. Zhou, *Sci. China-Technol. Sci.* **2024**, *67*, 311–320.
[45] J. Li, X. Miao, S. Wang, S. Chen, B. Han, G. Xu, K. Wang, B. An, D. Ju, W. Zhou, *Electrochemistry* **2022**, *90*, 077002.
[46] a) K. Cai, S.-H. Luo, J. Cong, K. Li, S.-X. Yan, P.-Q. Hou, Y. Song, Q. Wang, Y. Zhang, X. Liu, X. Lei, W. Mu, J. Gao, *J. Alloys Compd.* **2022**, *909*, 164882; b) C. Wang, Y. Zhao, L. Zhou, Y. Liu, W. Zhang, Z. Zhao, W. N. Hozzein, H. M. S. Alharbi, W. Li, D. Zhao, *J. Mater. Chem. A* **2018**, *6*, 21550–21557.
[47] a) F. Gao, L. Hou, S. Xiong, R. Cui, Y. Jiang, R. Chen, W. Liang, Z. Gao, *ChemElectroChem* **2021**, *9*, e202101447; b) Z. Z. Wang, J. Qu, S. M. Hao, Y. J. Zhang, F. Q. Kong, D. Yang, Z. Z. Yu, *ChemElectroChem* **2018**, *5*, 2653–2659; c) W. Zhao, Y. Yuan, P. Du, M. Zhu, S. Yin, S. Guo, *ChemElectroChem* **2021**, *8*, 3282–3293.
[48] K. Feng, M. Li, W. Liu, A. G. Kashkooli, X. Xiao, M. Cai, Z. Chen, *Small* **2018**,*14*, 1702737.
[49] a) H. Su, A. A. Barragan, L. Geng, D. Long, L. Ling, K. N. Bozhilov, L. Mangolini, J. Guo, *Angew. Chem. Int. Ed.* **2017**, *56*, 10780–10785; b) J. Zhuang, X. Xu, G. Peleckis, W. Hao, S. X. Dou, Y. Du, *Adv. Mater.* **2017**, *29*, 1606716.
[50] a) X. Ma, Y. Gao, M. Chen, L. Wu, *ChemElectroChem* **2017**, *4*, 1463–1469; b) W.-F. Ren, J.-T. Li, Z.-G. Huang, L. Deng, Y. Zhou, L. Huang, S.-G. Sun, *ChemElectroChem* **2018**, *5*, 3258–3265.
[51] J. Peng, R. Shao, S. Huang, Z. Cao, T. Zhang, Y. Cao, S. Zhang, C. Xu, Y. Shi, J. Niu, F. Wang, *J. Mater. Chem. A* **2022**, *10*, 23008–23014.
[52] C. Liu, M. Han, Y. Cao, L. Chen, W. Ren, G. Zhou, A. Chen, J. Sun, *Energy Storage Mater.* **2021**, *37*, 417–423.
[53] S. Zhou, J. Li, L. Fu, J. Zhu, W. Yang, D. Li, L. Zhou, *ChemElectroChem* **2020**, *7*, 2184–2189.
[54] J. Zhou, Q. Shi, S. Ullah, X. Yang, A. Bachmatiuk, R. Yang, M. H. Rummeli, *Adv. Funct. Mater.* **2020**, *30*, 2004648.
[55] X. Li, X. Han, R. Liu, S. Zhang, Y. Zhang, Y. Cao, X. Wang, R. Wang, Z. Yang, J. Sun, *Nanoscale* **2022**, *14*, 3625–3631.
[56] X. Liu, X.-Y. Wu, B. Chang, K.-X. Wang, *Energy Storage Mater.* **2020**, *30*, 146–169.
[57] Y. Chen, Y. Zou, X. Shen, J. Qiu, J. Lian, J. Pu, S. Li, F.-H. Du, S.-Q. Li, Z. Ji, A. Yuan, *J. Energy Chem.* **2022**, *69*, 161–173.
[58] G. Luo, X. Feng, M. Qian, W. Zhang, W. Qin, C. Wu, L. Pan, *Mater. Chem. Front.* **2023**, *7*, 3011–3036.
[59] L. Sun, T. Ma, J. Zhang, X. Guo, C. Yan, X. Liu, *Electrochim. Acta* **2019**, *321*, 134672.
[60] J. Zheng, Y. Wu, Y. Tong, Y. Sun, H. Li, *J. Colloid Interface Sci.* **2022**, *622*, 738–747.
[61] Y. Mu, D. Zhang, J. Li, B. Han, G. Xu, K. Wang, B. An, D. Ju, L. Li, W. Zhou, *Electrochim. Acta* **2022**, *437*, 141532.
[62] Y. Wu, Q. Pan, F. Zheng, X. Ou, C. Yang, X. Xiong, M. Liu, D. Hu, C. Huang, *J. Alloys Compd.* **2018**, *744*, 481–486.
[63] Y. Huang, R. Yu, G. Mao, W. Yu, Z. Ding, Y. Cao, J. Zheng, D. Chu, H. Tong, *J. Alloys Compd.* **2020**, *841*, 155670.
[64] B.-H. Hou, Y.-Y. Wang, Q.-L. Ning, C.-Y. Fan, X.-T. Xi, X. Yang, J. Wang, J.-P. Zhang, X. Wang, X.-L. Wu, *Nanoscale* **2019**, *11*, 1304–1312.
[65] S.-J. Liu, Z.-T. Wang, X.-H. Zhang, Z.-J. He, H. Tong, Y.-J. Li, J.-C. Zheng, *ACS Appl. Mater. Interfaces* **2020**, *12*, 2671–2678.
[66] D. Wu, Y. Ouyang, W. Zhang, Z. Chen, Z. Li, S. Wang, F. Wang, H. Li, L. Y. Zhang, *Appl. Surf. Sci.* **2020**, *508*, 145311.
[67] M. Ma, J. Zhang, W. Shen, S. Guo, *J. Solid State Electrochem.* **2019**, *23*, 2969–2977.
[68] H.-S. Jeong, H. Kim, K.-I. Jo, J. Jang, J.-H. Choi, J. Koo, *Appl. Surf. Sci.* **2020**, *508*, 144416.
[69] L. Möller, E. Thauer, A. Ottmann, L. Deeg, R. Ghunaim, S. Hampel, R. Klingeler, *J. Alloys Compd.* **2020**, *834*, 155018.
[70] W. Cao, A. Hu, X. Chen, X. Liu, P. Liu, Q. Tang, X. S. Zhao, *Electrochim. Acta* **2016**, *231*, 75–82.
[71] N. Zamani, A. R. Modarresi-Alam, M. Noroozifar, M. Javanbakht, *J. Appl. Electrochem.* **2019**, *49*, 327–340.
[72] A. Bahadur, S. Iqbal, M. Shoaib, *A. Saeed, Dalton Trans.* **2018**, *47*, 15031–15037.
[73] S. Iqbal, A. Bahadur, A. Saeed, K. Zhou, M. Shoaib, M. Waqas, *J. Colloid Interface Sci.* **2017**, *502*, 16–23.
[74] J. Bai, B. Zhao, X. Wang, H. Ma, K. Li, Z. Fang, H. Li, J. Dai, X. Zhu, Y. Sun, *J. Power Sources* **2020**, *465*, 228282.
[75] L. Luo, H. Yang, Z. Bai, D. Tao, S. Zhang, W. Xu, S. Sha, Q. Wei, *Ionics* **2018**, *24*, 297–301.
[76] K. Cao, H. Liu, X. Chang, Y. Li, Y. Wang, L. Jiao, *Adv. Mater. Technol.* **2016**, *2*, 1600221.
[77] B. Guan, W. Sun, Y. Wang, *Electrochim. Acta* **2016**, *190*, 354–359.
[78] J. Bai, B. Zhao, J. Zhou, J. Si, Z. Fang, K. Li, H. Ma, J. Dai, X. Zhu, Y. Sun, *Small* **2019**, *15*, 1805420.
[79] M. Yu, Y. Sun, H. Du, C. Wang, W. Li, R. Dong, H. Sun, B. Geng, *Electrochim. Acta* **2019**, *317*, 562–569.
[80] T. Zhao, Y. Zheng, Y. Meng, X. Huang, S. Chen, L. Chang, J. Shen, *J. Alloys Compd.* **2022**, *913*, 165279.
[81] S. Feng, J. Chen, L. Ma, J. Wu, J. Lin, L. Liao, X. Lu, X. Yan, S. Zeng, Y. Xi, *Ceram. Int.* **2022**, *48*, 20020–20032.
[82] Y.-R. Ji, S.-Y. Qi, J.-C. Wang, P.-F. Wang, N. Ren, T.-F. Yi, *J. Ind. Eng. Chem.* **2023**, *120*, 340–348.
[83] H. Zeng, B. Xing, C. Zhang, L. Chen, H. Zhao, X. Han, G. Yi, G. Huang, C. Zhang, Y. Cao, *Energy Fuels* **2020**, *34*, 2480–2491.
[84] M. Li, W. Ma, F. Tan, B. Yu, G. Cheng, H. Gao, Z. Zhang, *J. Power Sources* **2023**, *574*, 233146.
[85] Y. Teng, H. Zhao, Z. Zhang, Y. Li, H. Liu, *Mater. Lett.* **2019**, *246*, 141–143.
[86] H. Kim, W. Jae, J. Song, J. Kim, *J. Alloys Compd.* **2019**, *772*, 507–515.
[87] L. Kang, Z. Yang, W. Jiang, Y. Xu, Y. Meng, F. Wang, F. Liu, *React. Funct. Polym.* **2018**, *131*, 276–282.
[88] Q.-Y. Wei, H. Zhu, S.-J. Yu, G.-Q. Xu, J.-H. Yin, J.-H. Tong, T.-R. Chen, X.-N. He, P.-C. Guo, H.-D. Jiang, J.-K. Li, Y.-X. Wang, *Appl. Surf. Sci.* **2022**, *608*, 155093.
[89] M. Gao, S. Huang, Q. Zhang, G. Xu, Z. Chen, Y. Xiao, L. Yang, J. Cao, X. Wei, *ChemElectroChem* **2019**, *6*, 2891–2900.
[90] G. Luo, X. Feng, M. Qian, W. Zhang, W. Qin, C. Wu, L. Pan, *Mater. Chem. Front.* **2023**, *7*, 3011–3036.
[91] Y. Lu, Z. Ye, Y. Zhao, Q. Li, M. He, C. Bai, X. Wang, Y. Han, X. Wan, S. Zhang, Y. Ma, Y. Chen, *Carbon* **2022**, *201*, 962–971.
[92] J. Yan, C. Gao, S. Qi, Z. Jiang, L. R. Jensen, H. Zhan, Y. Zhang, Y. Yue, *Nano Energy* **2022**, *103*, 107779.
[93] X. Fan, T. Cai, S. Wang, Z. Yang, W. Zhang, *Small* **2023**, *19*, 2300431.
[94] X.-R. Wu, C.-H. Yu, C.-C. Li, *Carbon* **2020**, *160*, 255–264.
[95] J. Wang, C. Gao, Z. Yang, M. Zhang, Z. Li, H. Zhao, *Carbon* **2022**, *192*, 277–284.
[96] R. Amine, A. Daali, X. Zhou, X. Liu, Y. Liu, Y. Ren, X. Zhang, L. Zhu, S. Al-Hallaj, Z. Chen, G.-L. Xu, K. Amine, *Nano Energy* **2020**, *74*, 104849.
[97] X. Li, S. Zhang, J. Du, L. Liu, C. Mao, J. Sun, A. Chen, *Nano Res.* **2023**, *16*, 9273–9279.
[98] Y. Zhang, L. Wang, H. Xu, J. Cao, D. Chen, W. Han, *Adv. Funct. Mater.* **2020**, *30*, 1909372.
[99] M. Zhao, D.-L. Zhao, H.-X. Yang, X.-Y. Han, Y.-J. Duan, X.-M. Tian, W.-J. Meng, *Ceram. Int.* **2019**, *45*, 13210–13218.
[100] B. Wang, J. Jin, X. Hong, S. Gu, J. Guo, Z. Wen, *J. Mater. Chem. A* **2017**, *5*, 13430–13438.
[101] Y. Duan, S. Du, H. Tao, X. Yang, *Ionics* **2021**, *27*, 1403–1412.
[102] Y. Feng, K. Wu, H. Dong, X. Huang, C. Bai, J. Ke, D. Xiong, M. He, *Colloids Surf. A* **2020**, *602*, 125069.
[103] J. Oh, J. Lee, Y. Jeon, J. M. Kim, K.-D. Seong, T. Hwang, S. Park, Y. Piao, *ChemElectroChem* **2018**, *5*, 2098–2104.
[104] W. Ai, Z. Huang, L. Wu, Z. Du, C. Zou, Z. He, R. Shahbazian-Yassar, W. Huang, T. Yu, *Energy Storage Mater.* **2018**, *14*, 169–178.

[105] W. Luo, F. Li, J.-J. Gaumet, P. Magri, S. Diliberto, L. Zhou, L. Mai, *Adv. Energy Mater.* **2018**, *8*, 1703237.
[106] P. Feng, Z. Cui, S.-A. He, Q. Liu, J. Zhu, C. Xu, R. Zou, J. Hu, *J. Mater. Chem. A* **2019**, *7*, 24292–24300.
[107] J. Liu, L. Yu, C. Wu, Y. Wen, K. Yin, F.-K. Chiang, R. Hu, J. Liu, L. Sun, L. Gu, J. Maier, Y. Yu, M. Zhu, *Nano Lett.* **2017**, *17*, 2034–2042.
[108] Y. Cheng, Z. Yi, C. Wang, L. Wang, Y. Wu, L. Wang, *Chem. Asian J.* **2016**, *11*, 2173–2180.
[109] Z. Yi, Q. Han, P. Zan, Y. Wu, Y. Cheng, L. Wang, *J. Power Sources* **2016**, *331*, 16–21.
[110] K. Shen, Z. Zhang, S. Wang, Q. Ru, L. Zhao, L. Sun, X. Hou, F. Chen, *Energy Fuels* **2020**, *34*, 8987–8992.
[111] Z. Liu, S. Jin, K. Cui, J. Zhao, S. Xie, J. Li, C. Xinghua, *J. Alloys Compd.* **2020**, *842*, 155796.
[112] J. Yang, J. Xian, Q. Liu, Y. Sun, G. Li, *J. Energy Chem.* **2022**, *69*, 524–530.
[113] D. Zhou, W. L. Song, X. Li, L.-Z. Fan, *ACS Appl. Mater. Interfaces* **2016**, *8*, 13410–13417.

Manuscript received: September 26, 2023
Revised manuscript received: November 14, 2023
Version of record online: February 19, 2024